ELSEVIER

Ceramics International 31 (2005) 817–824

CERAMICS INTERNATIONAL

www.elsevier.com/locate/ceramint

Thermal shock properties and failure mechanism of plasma sprayed Al_2O_3/TiO_2 nanocomposite coatings

Chang-sheng Zhai[a,*], Jun Wang[a], Fei Li[a], Jing-chao Tao[a], Yi Yang[b], Bao-de Sun[a]

[a]*State Key Laboratory of Metal Matrix Composites, Shanghai Jiao Tong University, School of Materials Science and Engineering, 1954, Huashan Road, Shanghai 200030, PR China*

[b]*Henan Zhengzhou Dayang Thermal Spray Co. Ltd., Zhengzhou 45000, PR China*

Received 10 December 2003; received in revised form 16 July 2004; accepted 14 September 2004
Available online 15 December 2004

Abstract

Thermal shock properties and strengthening mechanics of Al_2O_3/TiO_2 nanocomposite ceramic coatings deposited by plasma spraying technology were studied. The results indicate that the thermal shock properties of plasma sprayed nanocomposite ceramic coatings get ahead of that of conventional Al_2O_3 and Al_2O_3/TiO_2 coatings. Presence of nanophase not only improves matching degrees of thermal propagation coefficient between ceramic coatings and bond-coats or substrates, but also lead cracks in top ceramic coatings to deviate, which could markedly prevent generation and propagation of thermal shock cracks. The study also shows that generation and propagation of thermal shock cracks locate at bond-coat/substrate interface. With the increase of thermal cycles, the thermal shock cracks propagate from bond-coat/TGO interface to top ceramic coat. The thermal shock temperature increase results in the reduction of thermal shock properties. The failure process of thermal shock includes crack initiation, propagation and coating spallation. Bond-coat/substrate interface is one of major factors which lead coatings to spallation failure.

Keywords: Nanocompsite coatings; Plasma spraying technology; Thermal shock properties

1. Introduction

Thermal sprayed Al_2O_3 and Al_2O_3/TiO_2 coatings are being extensively developed with many outstanding properties such as excellent abrasive and sliding wear resistance, erosion resistance, inoxidizability and heat-insulating property [1–3]. It is well known that, however, non-equilibrium γ-Al_2O_3 dominates the phase composition of the plasma sprayed coating. Intrinsic brittleness of ceramic materials and misfit of Young's modulus as well as thermal propagation coefficicient between ceramic coating and metal substrate lead to large residual stress in coating system, which often makes for spallation failure during thermal cycling process [3–6]. Existing researches indicate that functionally gradient structure from bond-coat to topcoat of thermal sprayed ceramic coating system helps to improve its thermal shock resistance [7–10]. Whereas, the method does not change intrinsic brittleness of top ceramic coat. At the same time, studies on nanocomposite materials demonstrate that nanophase-reinforced composite ceramic have better toughness and thermal shock resistance, other than those of conventional ceramic materials [11–16]. However, there were no reports that nanoparticles are used as reinforced phases to improve properties of thermal sprayed coatings to resist thermal shock.

In this paper, we prepared Al_2O_3/TiO_2 nanocomposite ceramic coatings were deposited by plasma spraying, and then researched thermal shock properties and strengthening mechanics of as-sprayed coatings.

* Corresponding author. Tel.: +86 21 62932870; fax: +86 21 62932914.
E-mail address: dannyeme@263.net (C.-s. Zhai).

0272-8842/$30.00
doi:10.1016/j.ceramint.2004.09.009

2. Experimental procedures

2.1. Processing

Both reconstituted Al_2O_3/TiO_2 nanocomposite powders with size range from 10 to 50 μm and Al/Ni alloy powders (Al, 20 wt.%; Ni, 80 wt.%; size range from 40 to 120 μm) were used for depositing coatings. The process of the reconstituted powders consist of spraying dry the slurry that contains 97 wt.% sub-micron α-Al_2O_3 (0.3–1 μm in diameter) and 3 wt.% nanostructured TiO_2 (5–80 nm diameter) particles, and subsequent heat treatment at high temperatures (800–1200 °C). All of the sub-micron Al_2O_3 powders, the nanostructured TiO_2 powders and the agglomerated particles were perfectly spherical in shape. The metal substrate was mild carbon steel (0.26% carbon content) with a diameter of 20 mm and length 5 mm.

Before the specimens were coated onto the plane of the substrate with a Al/Ni bond-coat (thickness 100 μm) and a Al_2O_3/TiO_2 nanocomposite ceramic coat (thickness 200 μm) deposited by APS, the substrate was sand-blasted with aluminum oxide grits to the surface roughness of Rz40 μm, and then cleaned in ultrasonic bath with acetone. The bond-coat and the ceramic top-coat were sprayed at the same condition. The substrate was preheated to about 200 °C before spraying.

The adopted plasma spray equipment includes: A Metco. 7 MB type and plasma spraying torch (made in Armored Force Engineering Institute, P.L.A, China) with inner-fed mode. The powder-injected position locates within the expanding segment of the anode-nozzle and the internal diameter of the anode-nozzle is 4 mm. Argon and H_2 were used as primary and the secondary plasma gases, respectively, whereas N_2 was used as the atomizing gas. The optimized parameters of plasma spraying are given in Table 1.

2.2. Thermal shock and characterization

The following steps constitute one thermal cycle: (□) the samples were heated to temperatures of 800 °C and 1000 °C in an automated furnace working in air, respectively. (□) the samples were quenched into water with a temperature of 25 °C after heat preservation for 15 min. The above steps were repeated. Each red-hot sample was observed visually during the cooling cycle. The occurrence of spallation, where the coatings falls off the metal substrate, is easy to discern. Delamination, where a portion of the coating is detached but is still hanging onto the substrate, results in a distinct change in contrast: the attached area appears dark whereas the detached area appears bright. A sample was considered to have failed when the coating failure area (spallation plus delamination) reached ~30% of the total coating area. Note that in this test both the substrate and the coatings are at the same temperature in the furnace.

As-sprayed coatings and thermal shock samples were characterized using a variety of techniques including X-ray diffraction (XRD), scanning electron microscopy (SEM), energy dispersive X-ray spectroscopy (EDS). X-ray diffraction was performed at a scanning rate of 1.5 deg/min on the samples using monochromatic Cu Kα radiation. Standard metallographic polishing techniques were used to prepare the cross-sectional samples.

Table 1
Plasma spray parameters for the reconstituted powders

Material	Reconstituted powders
Spray distance (mm)	60
Arc current (A)	360
Voltage (V)	85
Air flow rate ($m^3\ h^{-1}$)	1.8
H_2 flow rate ($m^3\ h^{-1}$)	0.4
Carrying gas flow rate ($m^3\ h^{-1}$)	1.0
Rotational speed of feeding wheel (rpm)	20

3. Results

3.1. Thermal shock properties of as-sprayed coating system

Fig. 1 compares the thermal cycling life of as-sprayed coatings at different temperatures. With the rising of thermal shock temperature, the average life of thermal cyclic fall down. Elevated temperature accelerates oxidation rate of substrate/bond-coat interface and thermal impact stress in inner of coatings. It was observed that thermal shock cracks came into being at substrate/bond-coat interface or specimen

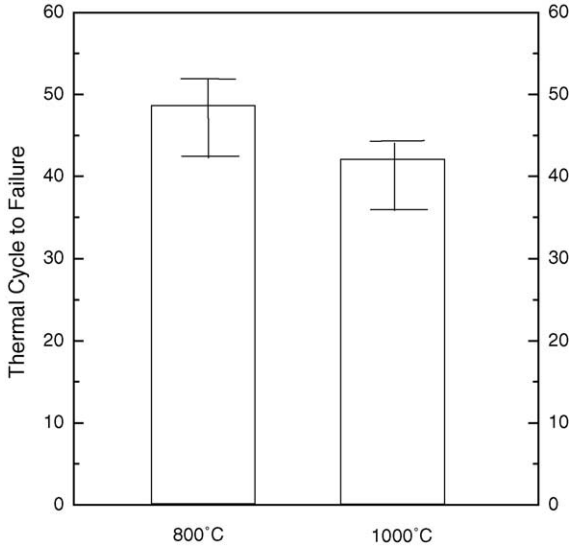

Fig. 1. Comparison of thermal cycling lives of as-sprayed coatings at different temperatures. Five specimens each were tested until failure. The histogram represents average values and the error bars represent minimum and maximum values.

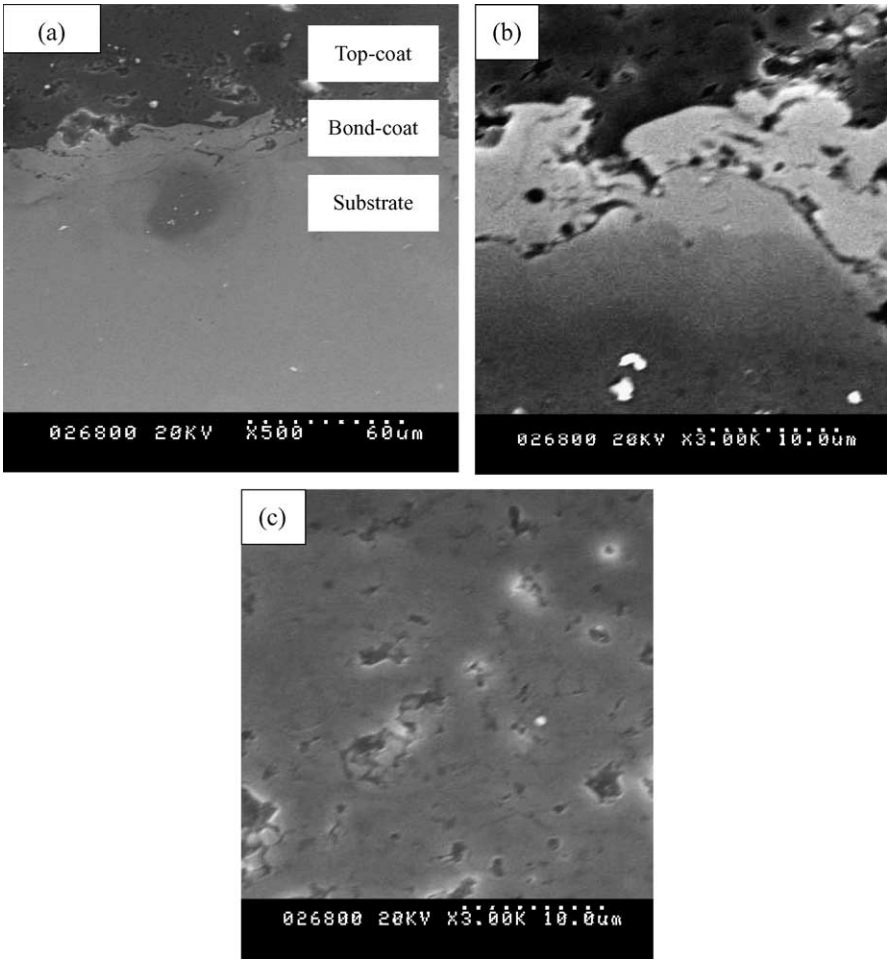

Fig. 2. SEM images of as-sprayed coatings in cross-section: (a) low magnified image and (b) high magnified image.

edge after certain thermal cycles. Due to action of thermal impact stress, cracks propagate along bond-coat/substrate interface leading to delamination and spallation. The results indicate that the thermal shock property of as-sprayed Al_2O_3/TiO_2 nanocomposite coatings gets ahead of that of conventional plasma sprayed Al_2O_3 and Al_2O_3/TiO_2 coatings [17–19]. Considering the new coatings are not optimized, these results are encouraging, with the potential for significant improvements in the durability of deposited Al_2O_3/TiO_2 nanocomposite coatings.

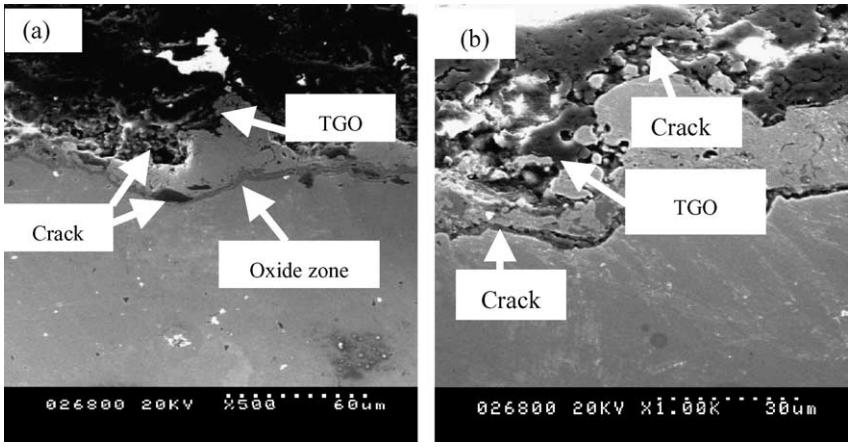

Fig. 3. SEM images of as-received coatings in cross-section: (a) after 20 thermal cycles and (b) after 50 thermal cycles.

3.2. Initiation and evolution of interface c

3.2.1. racks

Fig. 2 shows the microstructure of as-sprayed coating in cross section, with several feateurs of note. The coating is dense with a porosity of 2.7% and few pores with dimension of <10 μm. The typical laminated features can be seen in the cross-section, which was due to the peculiarity of the projective coating processes. There are no cracks in bond-coat interfaces with substrate and top-coat. EDAX indicates that there are no new oxidation products at the bond-coat and the interfaces between the substrate and the bond-coat.

With increased thermal cycles, new precipitates form on the grain boundaries, as shown in Fig. 3(a–b). Fig. 3 (a) indicates that the Al/Ni bond-coat boundaries form two oxidation-growing zones after 20 cycles from 800 °C to 25 °C. One zone locates in bond-coat/substrate interface where appears dark. EDAX indicates that the zone consists of abundant oxygen element, which shows that oxidation behavior occurs in the bond-coat/substrate interface, as presented in Fig. 4 (unmarked peak is Ag peak which was coated onto fracture surface of the sample for SEM analysis). At the same time, the iron element of the substrate diffuses against the grain boundary into the bond-coat. It is noted that EDS analysis of multi-dots in the bond-coat/substrate interface indicates average oxygen content at this interface is approximately 9%. The other zone locates in the bond-coat/top-coat interface, which is entitled thermally

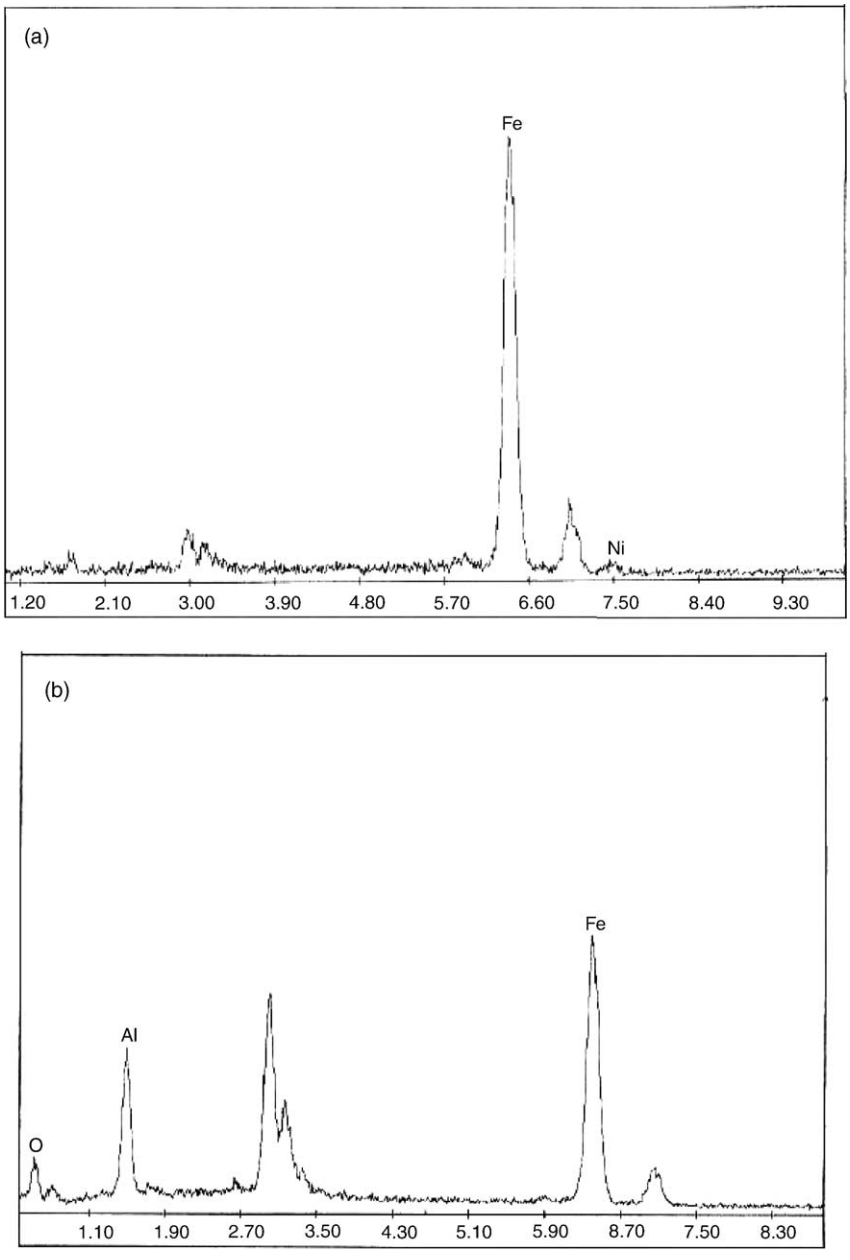

Fig. 4. EDAX for bond-coat/substrate interface of as-received coatings: (a) after spraying actually and (b) after 20 thermal cycles.

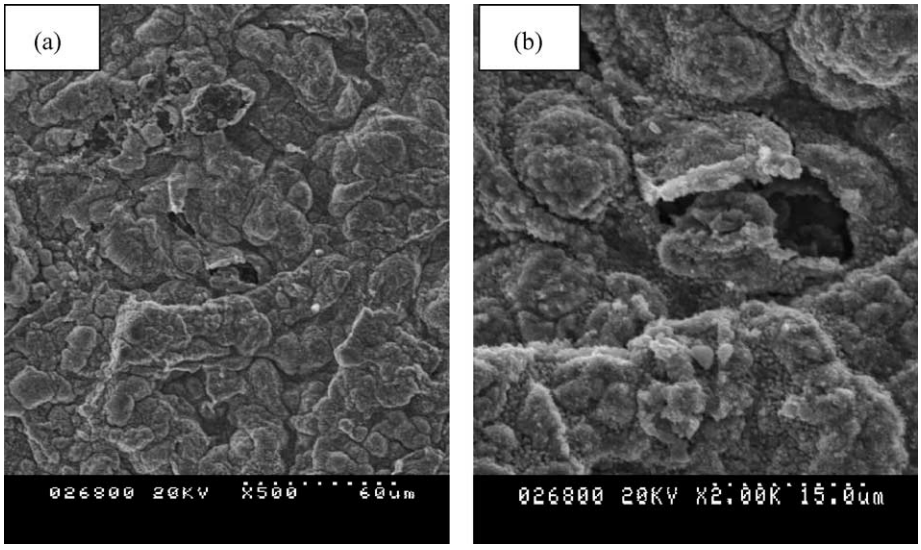

Fig. 5. Fracture morphology of thermal shock specimen after failure.

grown oxide layer (TGO). The TGO is essentially alumina oxide (Al_2O_3) [20–23]. Some initial cracks have come into being in the two zones.

Fig. 3 (b) shows microstructure features at bond-coat interfaces after 50 thermal cycles. The crack initiated at the very beginning of the thermal cycles. The cracks widened and propagated along the impression of the grain boundary of the bond-coat with increased cycles. At the same time, cracks in TGO propagated to topcoat, which illustrates that certain cracks of the top ceramic coat origin from TGO.

3.3. Microstructural characteristic of failure specimens

Fig. 5 (a) is a SEM micrograph of a cross-section Fracture surface of failed specimen at 800 °C. It revealed that failure Fracture mainly occurs at the bond-coat/substrate interface. The fracture surface is provided with rough structure, which illustrates heterogeneity of oxidation, thermal stress distribution and crack propagation perpendicular to bond-coat/substrate direction. Cauliflower structure of interface fracture is evident in the higher magnification SEM micrograph in Fig. 5 (b). Note the 3-D interpenetrating nature of interface structure, oxidation and crack propagation. X-ray diffraction characterization suggests that fracture phase are mainly oxidation and intermetallics in nature, as shown in Fig. 6. Intermetallics could be formed during thermal spraying process and maybe delay oxidation of bond coat, which is beneficial to improve the thermal shock resistance of as-sprayed coating system.

Fig. 7 shows surface morphology of failure specimen due to thermal shock. Certain macroscopic cracks were found in top ceramic coat, as presented in Fig. 7 (a). Propagation

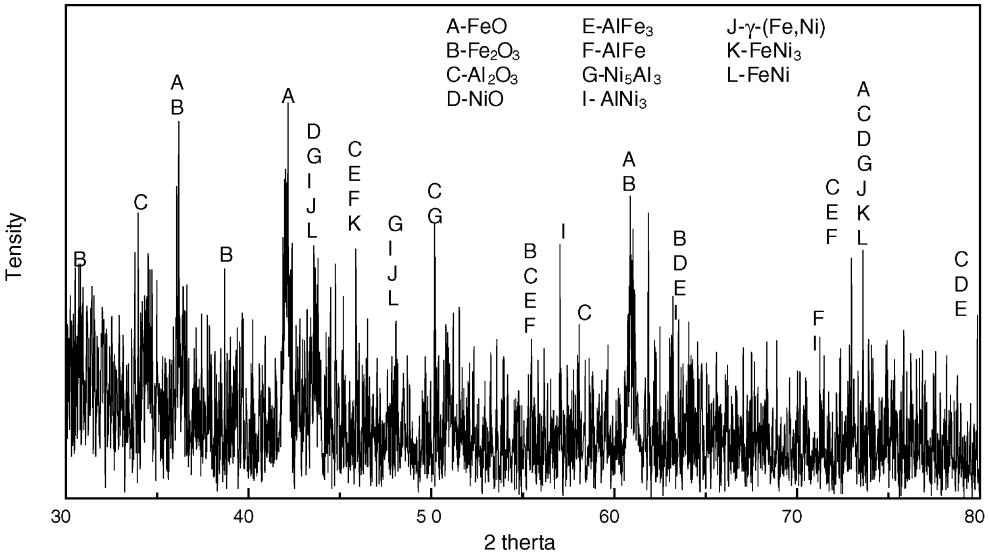

Fig. 6. Fracture phase of thermal shock specimen after failure (XRD).

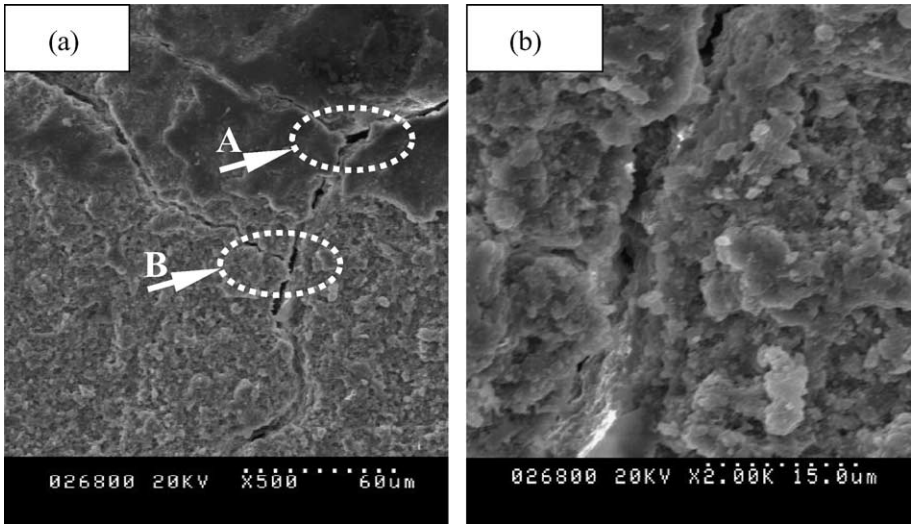

Fig. 7. Surface morphology of thermal shock specimen after failure.

direction of surface crack is perpendicular to each other at intersection point of cracks, as shown in A and B of Fig. 7 (a). Similar features were found at other positions of coating surface. Surface cracks could either origin from internal topcoat, or origin from surface flaws such as porosity and microcracks formed during deposition. Crack propagating plane takes on rugosity morphology, as in the higher magnification SEM imagine in Fig. 7 (b), which indicates cracks possibly deflect during propagateing process.

4. Disccusion

Under thermal cycling, thermal stress buildup and oxidation growth of the bond-coat interface with substrate and top coat could lead to interface imperfection such as interface undulation or asperity. Imperfections would result in redistribution of residual stresses and induce local tensile normal to the interface, large enough and over sufficient spatial extent to cause the formation of cracks. With increased thermal cycling, increased oxidation and propagateed cracks would lead to dramatic reduction of the bind strength of the bond-coat/substrate interface so as to make for further propagation of interface cracks and spallation failure along bond-coat/substrate interface of as-received coatings, which was companied by relaxation of the interface residential stress[24–26].

During thermal cycling, thermal growing oxidation (TGO) takes on critical effects to spallation at bond-coat/substrate, though final spallation failure does not occur at TGO or TGO/bond-coat interface. A schematic of cross-section of a thermal shock sample is shown in Fig. 8. As we know, TGO formed as a result of bond coat oxidation, is predominantly Al_2O_3 due to selective oxidation of Al element. Despite that TGO has a small thickness with few microns (as shown in Fig. 3), Al_2O_3 component of TGO is a

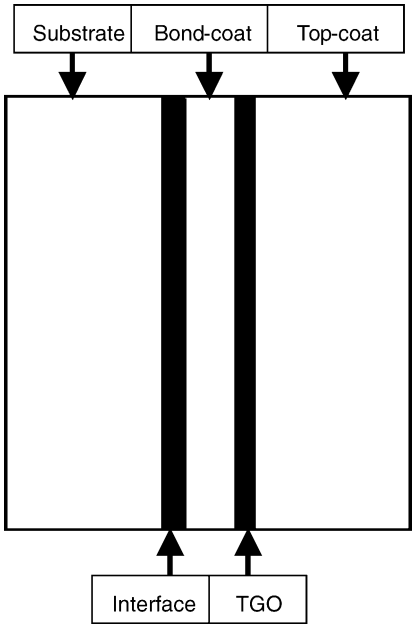

Fig. 8. A schematic of cross-section of a thermal shock sample.

ceramic material with more brittle and lower thermal propagation coefficient as well as thermal cycling resistance than top-coat, which increases misfit of physical proper with substrate and bond coat. Consequently, TGO would raise large thermal stress at substrate/bond-coat interface,

Table 2
Sintering point and thermal propagation coefficient of the related ceramic materials

Materials	Sinter point (K)	Coefficient of thermal propagation($\times 10^{-6}$ K)
Micro Al_2O_3	2073	8.3
Micro TiO_2	1646	6.8
Nanometer TiO_2	773	>13.6

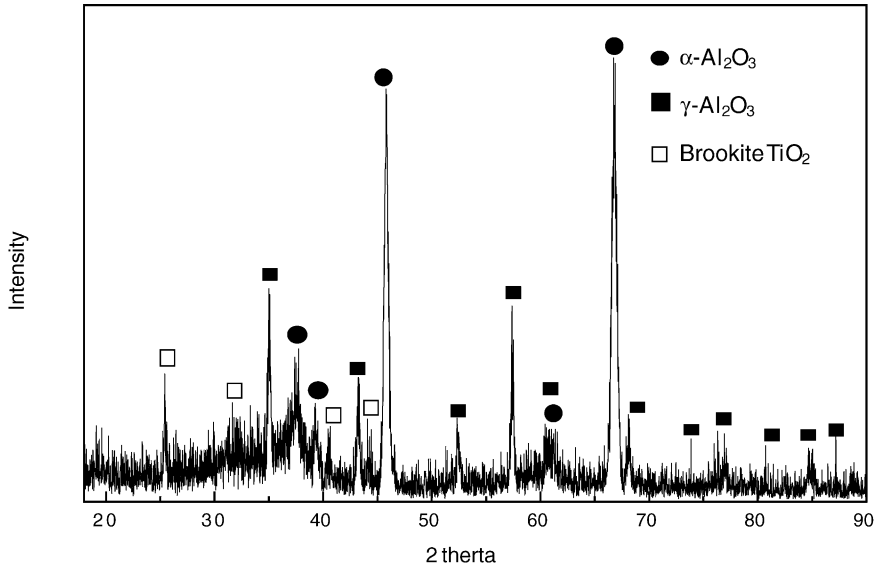

Fig. 9. Phase structure on ceramic layer of as-sprayed coating (XRD).

improving oxidation rate of bond coat and its delaminating rate from substrate. What's more, TGO is a multi-crack and mushy zone, thus cracks of TGO would rapidly propagate to top-coat during thermal cycling, resulting in top-coat failure. In one word, TGO plays a key role to spallation at bond-coat/substrate and failure of whole coating system. How to postpone formation and growth of TGO would markedly improve thermal shock resistance of coating system.

Despite that no significant differences in failure process were found between nano-reinfoced Al_2O_3/TiO_2 coating and conventional coating, the thermal shock property of former coating system overmatches that of the later [17–19], and the toughness mechanism of the former distinctly differs from the later. Improved thermal shock resistance could be attributed to nanoparticle reinforcement to the coating system.

Table 2 gives the sintering point and thermal propagation coefficient (CTE) of the nanometer TiO_2 and conventional ceramic materials [27,28]. Firstly, sintering point of nanometer TiO_2 material is remarkably lower than that of micro Al_2O_3 material. Other than conventional coatings, nanometer TiO_2 existence in as-sprayed ceramic agglomerates could make coatings deposited in low plasma spray power. So formation of metastable phase would be restrained to a great degree. The thermal stress in coating system and temperature of substrate would be reduced, which are beneficial to improve binding strength of coating system. Secondly, the thermal propagation coefficient of nanometer TiO_2 materials is more twice than that conventional TiO_2 materials and clearly higher than that of conventional Al_2O_3 materials [28]. Present of nanophase not only improves matching degrees of thermal propagation coefficient between ceramic coatings and bond-coats or substrates, but also build up ability of coating system to resist distortion. Therefore, initiation and propagation of thermal shock cracks could markedly be postponed.

Other than conventional Al_2O_3/TiO_2 coatings deposited by plasma spraying, there is no reaction product Al_2TiO_5 but α-Al_2O_3, γ-Al_2O_3 and brookite TiO_2 in as-sprayed coating, as shown in Fig. 9. According to toughness mechanism of nanocomposite ceramic materials [11–16], brookite TiO_2 could disperse in inner of ceramic coatings in the form of nanophase, which possibly bring a change of ceramic coating, from predominately intercrystalline structure to predominately transgranular structure. The structure not only effectively restrains exceptional growth of Al_2O_3 ceramic matrix granule, but also generates local stress due to propagation misfit of the two kinds of particles. According to the toughness of the nanocomposite materials [11–16], the addition of nanosized TiO_2 is also likely to lead to a change in the fracture mode of Al_2O_3 ceramic matrix during thermal cycling process, from predominately intergranular to predominately transgranular fracture, improving toughness of as-sprayed coating system. The unique structure and crack propagation mechanism could be nature to improve thermal shock performance of thermal spray nanocomposite ceramic coatings. It is also documented that thermal shock property of nanocomposite ceramic is higher than that of conventional ceramic. Further studies would be put up on microstructure and nature to resist thermal shock of thermal spray nanocomposite ceramic coating.

5. Conclusion

Plasma sprayed Al_2O_3/TiO_2 nanocomposite coatings have superior thermal cycling life. Improvement of thermal shock properties mainly depends on toughness mechanism other than conventional ceramic coatings. Compared with conventional Al_2O_3/TiO_2 coatings deposited by plasma spraying, there is no reaction product Al_2TiO_5 in as-sprayed coatings. TiO_2 dispersed in inner of ceramic coatings in the

form of nanophase. The addition of nanophase not only improves matching degrees of thermal propagation coefficient between ceramic coatings and bond-coats or substrates, but also possibly leads to a change in the fracture mode of Al_2O_3 ceramic matrix during thermal cycling process, from predominately intergranular to predominately transgranular fracture, improving toughness of as-sprayed coating system.

Presence of nanophase in Al_2O_3/TiO_2 agglomerates lowers plasma spaying power so as to reduce substrate temperature and non-equilibrium γ-Al_2O_3 content in as-sprayed coatings, which are beneficial to improve binding strength of coating system.

Initiation and propagation of thermal shock cracks locate at bond-coat/substrate interface. Along with thermal cycles increasing, the thermal shock cracks propagate from bond-coat/TGO interface to top ceramic coat. The thermal shock temperature increment results in falling of thermal shock properties. The inactivation process of thermal shock includes crack initiation, propagation and coating spallation. Bond-coat/substrate interface is one of major factors lead coatings to spallation failure.

Al_2O_3 component of TGO increases misfit of physical property with substrate and bond coat and has low thermal cycling resistance. So TGO takes on critical effects to final spallation at bond-coat/substrate.

Acknowledgements

The authors would like to express their appreciation to the Nanotechnology fundation of Shanghai (No. 0352mm054). The authors also thank Mrs. N. H. Xu for both the use of Scanning Electron Microscope and her insight and tireless work.

References

[1] You Wang, Stephen Jiang, Meidong Wang, Shihe Wang, T. Danny Xiao, Peter R. Strutt, Wear 37 (2000) 176–185.
[2] E.H. Jordan, M. Gell, Y.H. Sohn, D. Goberman, et al., Mater. Sci. Eng. A 301 (2001) 80–89.
[3] D. Goberman, Y.H. Sohn, L. Shaw, E. Jordan, M. Gellm, Acta Mater. 50 (2002) 1141–1152.
[4] E. Tzimas, H. Mullejans, S.D. Peteves, J. Bressers, W. Stamm, Acta Mater. 4 (8) (2000) 4699–4707.
[5] R. Ahmed, M. Hadfield, Wear 220 (1998) 80–91.
[6] Xiangyang Jiang, Yuepeng Wan, Herbert Herman, Sanjay Sampath, Thin Solid Films 385 (2001) 131–141.
[7] K.W. Schlichting, N.P. Padture, E.H. Jordan, M. Gell, Mater. Sci. Eng. A 342 (2003) 120–130.
[8] Chungen Zhou, Jingsheng Yu, Shengkai Gong, Huibin Xu, Surf. Coatings Technol. 161 (2002) 86–91.
[9] A. Kawasaki, R. Watanabe, Fract. Mech. 69 (2002) 1713–1728.
[10] Y.P. Wan, S. Sampath, V. Prasad, R. Williamson, J.R. Fincke, J. Mater. Process. Technol. 137 (2003) 110–116.
[11] T. Sekimo, K. Niihara, Nanostruct. Mater. 6 (1995) 663–666.
[12] Kwang-Taek, Chang-sam Kim, Kuen-Ho Auh, et al., Mater. Lett. 32 (1997) 251–257.
[13] Hyoung Joon Park, Hyoun-Ee Kim, Koichi Niihara, J. Eur. Ceram. Soc. 18 (1998) 907–914.
[14] T. Hirano, K. Izaki, K. Niihara, Nanostruct. Mater. 5 (1995) 809–818.
[15] Noriko Bamba, Yong-Ho Choa, Tohru Sekion, Koichi Niihara, J. Eur. Ceram. Soc. 18 (1998) 693–699.
[16] K. Niihara, J. Ceram. Soc. Jpn. 99 (1999) 974–982.
[17] Li Muqin, Ma Chen, Welding Trans. 18 (1997) 6–11.
[18] A. Ramaswany, S. Seetharamu, K.B.R. Varma, et al., Comp. Sci. Tech. 57 (1997) 81.
[19] S. Bourban, N. Karapalis, H. Hofmann, et al., Acta Mater. 45 (1997) 5069.
[20] J.A. Thompson, T.W. Clyne, Acta Mater. 49 (2001) 1565–1575.
[21] M.J. Pindera, J. Aboudi, S.M. Arnold, Mater. Sci. Eng. A 284 (2000) 158.
[22] Z.A. Chaudhury, G.M. Newaz, S.Q. Nusier, et al., J. Mater. Sci. 34 (1999) 2475.
[23] N.P. Padture, K.W. Schlichting, T. Bhatia, et al., Acta Mater. 49 (2001) 2251–2257.
[24] K. Kokini, M. Case, ASME J. Eng. Mater. Technol. 119 (1997) 148–152.
[25] Y.D. Lee, F. Erdogan, Int. J. Fract. 69 (1995) 145–165.
[26] K. Miyawaki, T. Hashida, H. Takahashi, J. Jpn. Soc. Powder Metall. 37 (7) (1990) 957–961.
[27] Lide Zhang, Jimei Mu, Nanophase Materials and Nanophase Structure, Science Press, Beijing, 2001.
[28] Zhenze Guan, Zhongtai Zhang, Jinsheng Jiao, Physical Property of Organic Material, Tsinghua University Press, Beijing, 1992.